ACS Sustainable Chemistry & Engineering

Research Article

pubs.acs.org/journal/ascecg

Natural Nanotube-Based Biomimetic Porous Microspheres for Significantly Enhanced Biomolecule Immobilization

Cong Chao,[†] Bing Zhang,*[,†] Rui Zhai,[†] Xu Xiang,*[,‡] Jindun Liu,[†] and Rongfeng Chen[†]

[†]School of Chemical Engineering, Zhengzhou University, Zhengzhou, 450001, P.R. China

[‡]State Key Laboratory of Chemical Resource Engineering, Beijing University of Chemical Technology, Beijing, 100029, P.R. China

Supporting Information

ABSTRACT: Inorganic nanostructures and their assemblies play important roles in immobilizing biomolecules. Herein, we developed a facile and green methodology to assemble natural halloysite nanotubes (1D building blocks) into nest-like porous microspheres (3D architecture). We further modified the microspheres with dopamine to form a biomimetic entity. The interconnected and hierarchical pores within the microspheres provide larger pore volume to entrap biomolecules, and the abundant functional groups on the pore surface bond covalently with enzyme to enhance the immobilization ability. The porous microspheres showed excellent loading capacity for laccase immobilization as high as 311.2 mg/g, around 30 times higher than the individual halloysite nanotubes (11.3 mg/g). The specific activity above 80% was retained for the immobilized laccase compared to the free laccase. In addition, the immobilized enzyme exhibited remarkable thermal and recycle use stability. The biomimetic microspheres are expected to be biologically safe and chemically stable microcapsules for immobilizing a variety of biomolecules because of their natural and biofriendly characteristics.

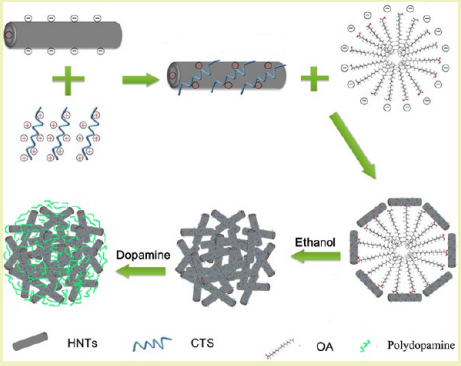

KEYWORDS: *Halloysite, Natural nanotubes, Self-assembly, Porous microspheres, Dopamine, Enzyme immobilization*

INTRODUCTION

Silicate minerals, as pervasive compounds in the earth's crust, can exist in different morphologies, such as nanoplates (kaolinite), nanotubes (chrysotile, imogolite, and halloysite), and nanorods (palygorskite), which are natural and abundant nanomaterials for versatile applications.[1−5] Among the minerals, halloysite ($Al_2Si_2O_5(OH)_4 \bullet nH_2O$), a naturally forming two-layered aluminosilicate with a hollow nanotubular structure, consists of one alumina octahedron sheet and one silica tetrahedron sheet in a 1:1 stoichiometric ratio (Figure 1). The external surface is composed of siloxane (Si−O−Si) groups, whereas the internal surface consists of a gibbsite-like array of aluminol (Al−OH) groups. The different chemical constitutions determine the negatively charged outer surface and positively charged inner lumen within a certain pH range.[6−8] The environmental friendly and biocompatible nature enables halloysite nanotubes (HNTs) to be a promising nanomaterial for developing organic/inorganic composites in the biomedicine field.[9−12] Compared with several traditional silicate supports with small pore sizes of 0.3−2 nm (roughly the same size as small molecules), such as intercalated clay and montmorillonite,[13,14] HNTs with an inner diameter of 5−20 nm are more suitable candidates to entrap biomacromolecules or achieve controlled release of drugs.[15−17]

Halloysite nanotubes, like many other nanotubes, have a tendency to form bundles or agglomerates, which result in a reduction in effective specific surface area. Therefore, the performance for biomolecules immobilization would be severely hindered.[18−20] To address this issue, one effective and facile approach is self- and/or directed assembly of these

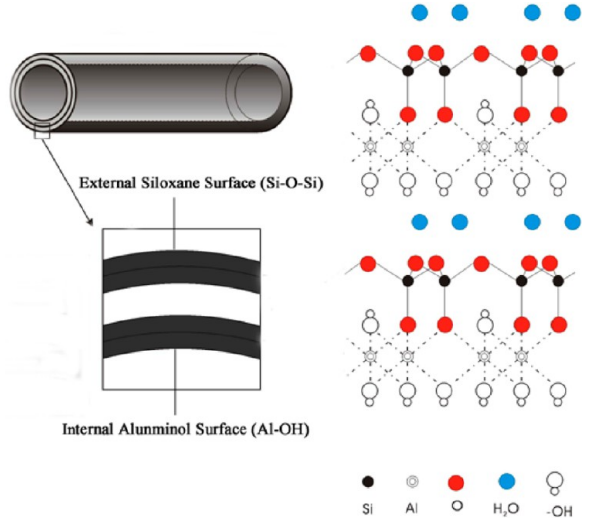

Figure 1. Illustration of the composition and structure of a halloysite nanotube.

Received: June 26, 2013
Revised: July 22, 2013
Published: July 31, 2013

nanoscale building blocks into three-dimensional (3D) microporous structures.[18−23] Therefore, the hierarchical structure can take the advantages of both nanosized building blocks and micro- or submicrosized assemblies. The 3D hierarchical pores could enhance the accessibility of immobilized enzymes or biomolecules to substrates during the reactions by reducing or eliminating mass-transfer barriers of reactants. Compared with other nanosized materials, few studies have been reported on the self-assembly of halloysite nanotubes.[24] To assemble natural halloysite nanotubes into hierarchical porous structures still remains a highly challenging task.

Recently, a variety of supports modified with dopamine has been studied for biomolecules immobilization.[25−29] Dopamine, a biomolecule that contains catechol and amine functional groups, can self-polymerize in weak alkaline solutions and spontaneously deposit polydopamine conformal films on virtually any surface. The abundant functional groups (i.e., catechol and amine) existing on the modified surface can enhance the binding ability for various biomolecules. On the basis of this mechanism, we modified dopamine onto the surface of the product to form a new biocmpatible support for immobilizing enzymes or biomolecules.

In recent years, some biological structures have provided inspiration for groups trying to design and fabricate new functional structured materials with exceptional properties and functionalities.[30,31] Inspired by the swallow nest-like structure made from straws, mud, and its saliva, in the present work, we chose kind of natural nanotubes as building blocks, self-assembled them into nest-like porous microspheres (3D architecture) through a facile wet chemistry method, and further modified microspheres with biomolecules of dopamine to strengthen the biomimetic entity. While the porous microspheres were used as supports for biomolecule immobilization, they displayed superiority over other synthetic supports. The preparation of microspheres can be scalable and green owing to the abundant resource of halloysite and the mild procedure, in which no toxic agents were involved.

EXPERIMENTAL SECTION

Materials. The halloysite mineral was obtained from Henan province, China. After milled and sieved with a 75 μm sieve, the halloysite mineral was dispersed in water to form a colloidal suspension. The suspension was further spray dried to obtain a fine powder at 473 K. The compositions of halloysite powder were determined by chemical analysis. The halloysite powders consist of 46.16% SiO_2, 38.70% Al_2O_3, 0.033% MgO, 0.191% CaO, 0.05% Fe_2O_3, 0.03% K_2O, 0.04% Na_2O, 0.004% TiO_2, and 14.60% loss on ignition.

Laccase from *Trametes versicolor* (EC 1.10.3.2, 13.6 U mg^{-1}), urease, horseradish peroxidise, 2,2-azinobis-3-ethylbenzothiazoline-6-sulfonate (ABTS, 99%), and fluorescein isothiocyante (FITC) were purchased from Sigma-Aldrich (USA). All other chemicals were of analytical grade and were used without further purification.

Preparation of Porous Microspheres. In a typical synthesis, a dispersion of HNTs in deionized water (4 wt %) was stirred thoroughly and homogenized in an ultrasonic bath for 1 h. Chitosan (1.4 wt %) was dissolved in an aqueous solution of glacial acetic acid (2 wt %). The same volume (50 mL) of the HNTs solution and chitosan solution were mixed under constant stirring to guarantee full adsorption of chitosan on HNTs. The chitosan-coated HNTs solution was emulsified with oleic acid (OA, 25.0 mL), a biocompatible organic phase, to form a water/oil microemulsion. After being left to rest for 12 h, ethanol solution was added into the mixture to break the microemulsion and form precipitate. Then the precipitate was neutralized by NaOH solution and repeatedly rinsed with distilled deionized water until a neutral pH was achieved. Finally, the precipitate was dipped in a dopamine buffer solution of tris-(hydroxymethyl) aminomethane (0.4 mg/mL, pH 7.5) for 6 h. The resulted black product was separated by centrifugation and washed with distilled water repeatedly.

Characterization. The microstructures of the samples were observed using a transmission electron microscope (TEM, FEITEC-NAIG2) and scanning electron microscopy (SEM, JSM-7500F). The surface potential of the halloysite at different pH levels was measured by the microelectrophoretic method using the Malvern Zetasizer Nano ZS apparatus. The size distribution of microspheres was measured by a dynamic light scattering technique on a laser particle size analyzer (Malvern, Mastersizer 2000). The FTIR spectra were recorded at room temperature with a Bruker Vector 22 spectrometer in the range 4000−400 cm^{-1} at a 2 cm^{-1} resolution. X-ray photoelectron spectra (XPS) were recorded on a Thermo VG ESCALAB250 X-ray photoelectron spectrometer at a pressure of about 2×10^{-9} Pa using Al Kα X-ray as the excitation source (1486.6 eV). The shifts of all binding energies were calibrated using a C1s core level at 284.6 eV. The measurements of specific surface areas were performed by a BET method from N_2-adsorption measurements at 77 K using a Quantachrome NOVA 2000e surface area and pore size analyzer. The mercury intrusion analysis was performed on a AutoPoreIV 9510 porosimeter from Micromeritics to determine macropores distribution.

Immobilization of Enzyme. The immobilization of laccase (1.15 mg/mL) was carried out by incubating the microspheres in the citrate−phosphate buffer (2 mL, 0.1 M, pH 6.8) containing various amounts of laccase at 4 °C for 24 h. After immobilization, the solid microspheres were washed three times with the buffer to remove nonspecific-adsorbed laccases, and the supernatants were collected. The immobilized enzymes were stored at 4 °C prior to use. The supernatant was used to measure the concentration of the residual enzyme to determine the enzyme loading on the microspheres. The enzyme concentration in the collected supernatant was determined by measuring its initial catalytic reaction rates with substrates. The enzyme loading is defined as the difference between the total enzyme used and the residual enzyme in the supernatant after immobilization.

Determination of Enzyme Activity. The activity of free or immobilized enzyme was measured using a colorimetric assay with ABTS as a color-generating substrate, where the rate of color formation was proportional to enzyme activity.[30] The dilute enzyme (100 μL) was added in a 2 mL assay mixture consisting of 0.25 mM of ABTS and 100 mM of citrate−phosphate buffer at pH 4.2. The formation of a ABTS-cation radical ($ABTS^{\bullet}$) in the assay due to the catalytic action of laccase was monitored at a wavelength of 420 nm using a UV−vis spectrophotometer (Shimadzu, UV-3000) and an extinction coefficient of 36 mM/cm^{-1}. One unit of enzyme activity (U) was defined as the amount of enzyme that converted 1 μmol of ABTS to $ABTS^{\bullet}$ per minute at 30 °C. The enzyme activity assay was always performed in triplicate, and the standard deviations in measurements were consistently below 3%.

RESULTS AND DISCUSSION

The morphologies of the natural HNTs were characterized by SEM and TEM (Figure 2). The SEM image shows the general morphology of HNTs (Figure 2a). No particles or other nanostructures were found in the SEM observation, indicating that the product consists of pure nanotubes. The image of TEM shows that the HNTs have clearly hollow tubular structures (Figure 2b). The HNTs have lengths ranging from 0.5 to 1 μm, diameters in the range of 40−60 nm. The distinct morphology shows nanotubes have a good dispersion. The typical XRD pattern of the HNTs is shown in Figure S1 of the Supporting Information. The diffraction peaks can be indexed to the hexagonal structured ($Al_2Si_2O_5(OH)_4 \bullet 2H_2O$), which are in agreement with the reported values of halloysite: 7 Å with lattice constants of a = 5.13 and c = 7.16 (JCPDS card no. 29-1487). The significant broadening of the diffraction peaks is ascribed to the small crystallite size. The zeta potential of

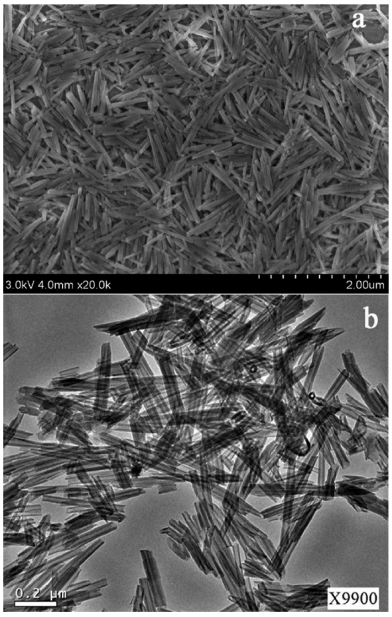

Figure 2. SEM and TEM photograph of halloysite nanotubes (HNTs).

HNTs was determined from pH 2.2−11.0 (Figure S2, Supporting Information). The pH_{zpc} of HNTs was found to be ∼2.3, which is similar to the results reported by Levis and Mellouk.[33,34] The surface of the HNTs is negatively charged above pH 2.3, which offers a possibility for adsorption of some positive macromolecules on the surface.

The self-assembly for the microspheres includes four steps (Figure 3). First, chitosan (CTS), a polycationic polysaccharide,[35] could effectively be bonded to the negatively charged outer surface of HNTs to form a positively charged CTS-HNTs assembly. Second, the aqueous suspension containing CTS-HNTs is emulsified by oleic acid (OA). It is known that surfactant molecules can form micelle self-assembly above the critical micelle concentration, which is usually utilized as a soft template for synthesis of nanostructures.[36] Here, OA, an amphiphilic molecule, forms micelles with hydrophilic heads outward and hydrophobic tails interwoven in an oil/water system. The individual CTS-HNTs are attached to negatively charged hydrophilic heads of OA, resulting in an OA-encapsulated structure. CTS-HNTs form aggregates outside via the electrostatic interaction and large oil/water surface energy, which is larger than the difference between the nanotube−oil and nanotube−water surface energies.[37,38] Third, after the oil droplet is completely covered by the CTS-HNTs, the structure is transferred into an ethanol medium. The oil core was dissolved into the ethanol and the shell, consisting of CTS-coated HNTs, aggregated to form microspheres. Finally, dopamine was further modified onto the surface of the microspheres, which is a catechol derivative inspired by wet adhesion systems developed by nature.[25−29]

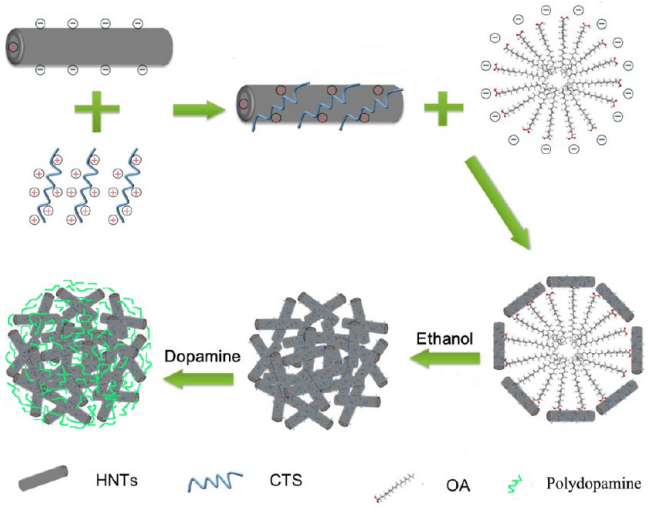

Figure 3. Illustration of self-assembly of the halloysite nanotubes into biomimetic porous microspheres.

The microspheres in wet state were examined by an optical microscope, as shown in Figure 4a. The photograph confirms that the microspheres have a size distribution ranging from 10 to 30 μm. This size distribution is verified by analyzing the diameters of microspheres using a particle size analyzer. The microspheres show a size distribution centered at 22 μm (Figure 4b), consistent with the result optically observed.

To examine the fine morphology, microspheres were also observed by scanning electron microscopy (SEM). Figure 5 shows the SEM images of the microspheres unmodified (Figure 5a,b) and modified with dopamine (Figure 5c,d). Figure 5a shows that the natural halloysite nantubes can self-assemble into a nest-like porous microspheres. This is ascribed to the electrostatic attraction among the chitosan-coated HNTs and the hydrophilic heads of OA molecules in a microemulsion. It is noted that the size of microspheres (in the range of ∼20−25 μm) is much larger than that of an individual micelle of OA (several tens of nm).[36] Therefore, the formation of microspheres is involved in assembly from hundreds of self-assembled OA-micelle-encapsualted structure. The HNTs keep their intrinsic tubular structure and overlap each other (Figure 5b). By contrast, the microspheres are slightly altered after the modification of dopamine, in which the nanotubes have a tendency to form bundles (Figure 5c). Moreover, the surface of microspheres after modification becomes rougher (Figure 5d), which can be attributed to the attachment of polydopamine.[39]

The surface area and pore size distribution were revealed by N_2 adsorption/desorption measurements (Figure S3, Supporting Information). The microspheres exhibit a higher BET surface area (114.6 m^2/g) and larger pore volume (0.347 cm^3/g) than pristine HNTs (59.6 m2/g) and (0.238 cm^3/g), respectively (Table S1, Supporting Information). The pore size shows a wide distribution from mesopores to larger pores. A minor peak is also observed at the pore size about 4 nm. The mercury porosimetry measurement indicates that the microspheres have a continuous pore distribution from mesopore extending to macropore region (∼250 nm) (Figure S4, Supporting Information). For biomolecule immobilization, larger pore size in the supports is of great importance.[21] The hierarchical and interconnected pore distribution in the microspheres may be more beneficial to the mass transfer of reactants and products over other porous supports (e.g., zeolites). In the current case, the larger pores are advantageous to enzyme immobilization or entrapment. Therefore, the pore distribution within the microspheres could be attributable to the interparticle space of the nanotubes except for the contribution from the lumen space of HNTs. Takahara et al. found that the dopamine derivatives could selectively function-

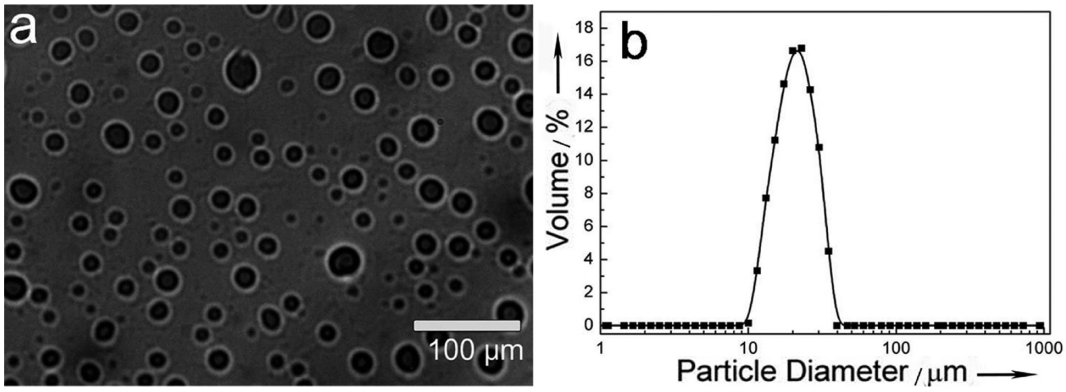

Figure 4. (a) Optical microscope image and (b) particle size distribution of the microspheres measured by a particle size analyzer.

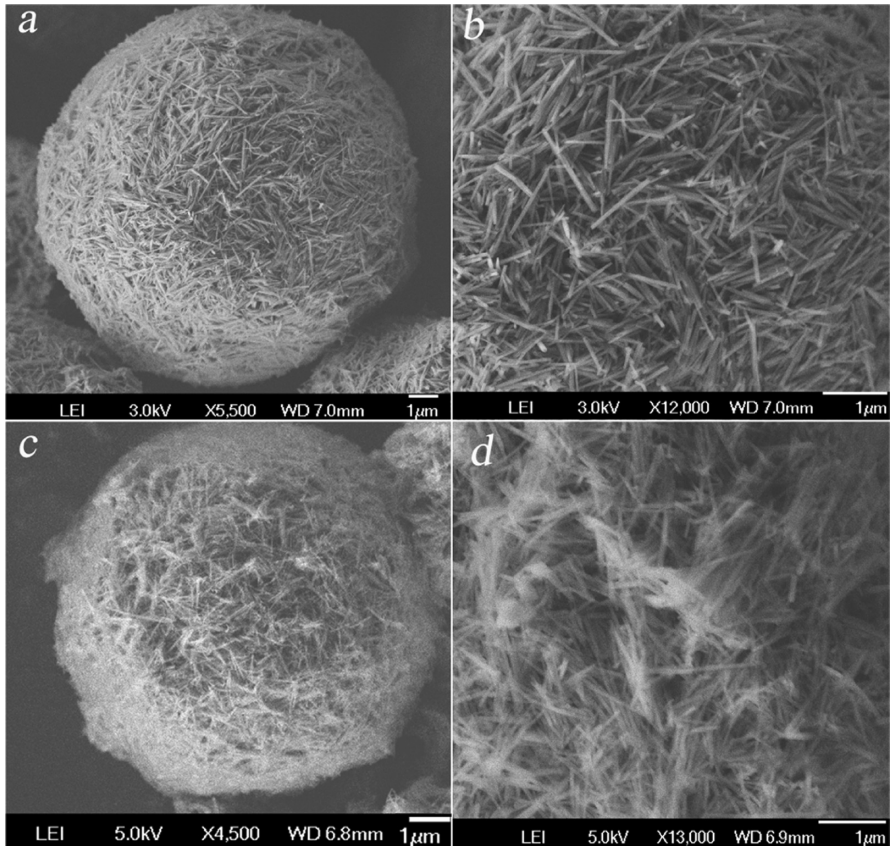

Figure 5. SEM photographs of the microspheres before (a) and after (b)modification of dopamine (c) and (d).

alize the lumen of HNTs due to a strong catechol−alumina interaction in the halloysite lumen.[26] Compared to the pore size of the pristine HNTs (a mean pore size of ∼21 nm), the results from N_2-adsorption or mercury porosimetry measurements reveal that the porous microspheres have a smaller mean pore size within the mesopore range. This indicates that polydopamine could modify the lumen surface of halloysites and lead to a decrease in the size of lumen.

Dopamine can self-polymerize at an alkaline solution and spontaneously deposit poly(dopamine) conformal films on virtually any surface.[25−29] It is commonly believed that catechol groups were oxidized to quinone form in alkaline conditions, although the polymerization mechanism of dopamine on the surface of supports is not explicitly demonstrated so far.[25−29] The cross-linking of poly(dopamine) was ascribed to the reverse dismutation reaction between catechol and o-quinone form.[27,28,40−44] The XPS survey spectra of the microspheres show the additional presence of C and N (Figure 6), compared with the spectra of the pristine HNTs (Figure S5, Supporting Information). The N/C ratio is 0.084, which is lower than the theoretical value of dopamine (N/C = 0.125). This may be explained by the effect of CTS, which has a lower N/C ratio than dopamine. The Si and Al elements from HNTs are also detected by XPS. It is mostly ascribed to the ultrathin assembly of dopamine (about several nanometers) onto the HNTs in terms of the detection depth of XPS. The signals could also result from the exposed surface of halloysite nanotubes. The complicated nature of poly(dopamine) on the microspheres was revealed by the different chemical states of elemental C, O, and N in deconvoluted core level spectra (Figure 6). The C1s

dx.doi.org/10.1021/sc400199v | ACS Sustainable Chem. Eng. 2014, 2, 396−403

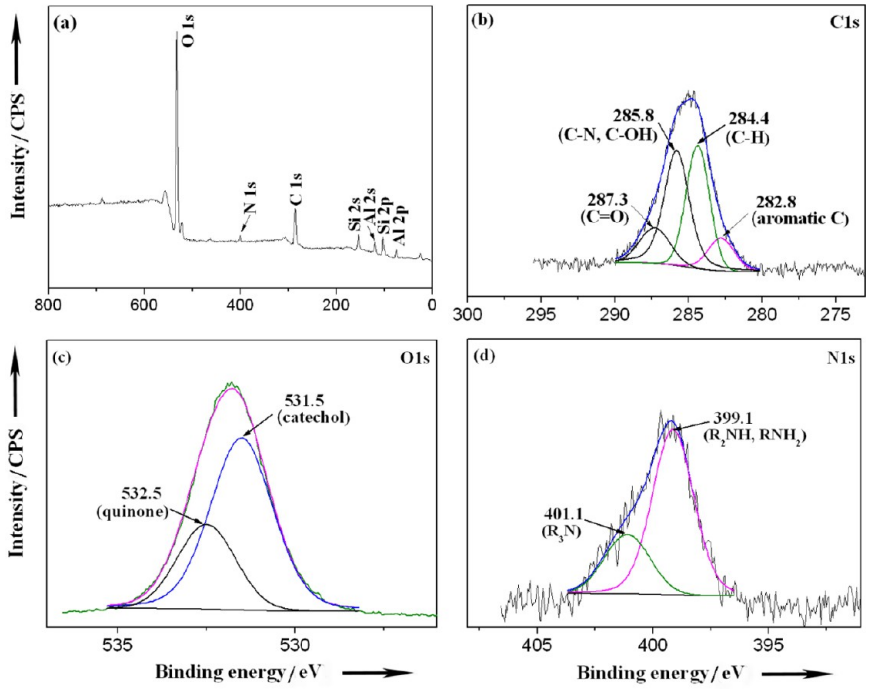

Figure 6. High-resolution XPS spectra of the microspheres (a) survey, (b) C1s, (c) O1s, and (d) N1s core level.

spectra can be deconvoluted into four fitted peaks, corresponding to aromatic carbon in dopamine structure (282.8 eV), C−H bond (284.4 eV), C−N (285.8 eV), and C═O group (287.3 eV), respectively. The deconvoluted O1s spectra show two peaks centered at 531.5 and 532.5 eV, which are assigned to the catechol and quinine forms in dopamine. This reveals that the initial catechol group is partially transformed into quinine forms after functionalization. The N1s spectra displays two deconvoluted peaks at 399.1 (primary amines/secondary amines) and 401.1 eV (tertiary amines), consistent with the literature reported for dopamine-modified solid surfaces.[45] The residual quinones in the surface, which are reactive toward nucleophilic amino groups, can give rise to covalent linking to nucleophilic biomolecules through the Michael addition and/or Schiff base formation.[42,43]

The loading capacities of the porous microspheres were investigated through incubating the supports in laccase solution with various concentrations. The laccase loading on the support increased with its initial concentration (Figure 7). When the concentration of laccase increased to 3.5 mg/mL, the loading on the microspheres reached as high as 311.2 mg/g, 30 times higher than that on pristine HNTs (11.3 mg/g). The capacity was an order of magnitude higher than the previously reported porous supports, such as nanoporous gold (15.5 mg/g), CTS (20 mg/g), sepabeads EC-EP3 (32.6 mg/g), magnetic mesoporous silica spheres (82 mg/g), and MMSNPs-CPTS-IDA (98.1 mg/g).[35,46−49] Such a high loading capacity can be partially attributable to the increased surface area of the microspheres compared to the pristine HNTs (114.6 vs 59.6 m^2/g) and a wide pore size distribution. In addition, the high capacity for laccase loading could be attributable to the homogeneous modification of poly(dopamine) on the exterior surface and/or inner lumen of the microspheres, which introduces abundant functional groups to effectively bind laccase within the pores of the microspheres and inner lumen of the nanotubes.[26] The microspheres also exhibit high loading ability for other enzymes, such as urease (256.3 mg/g) and

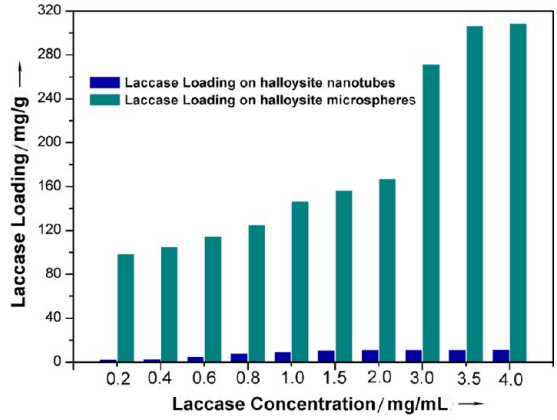

Figure 7. Laccase loading on pristine HNTs and porous microspheres at different initial concentrations.

horseradish peroxidise (295.6 mg/g), indicating that its generality for biomolecule immobilization.

The retention of high activity in the immobilized enzymes is required for their practical applications. To evaluate the activity of the immobilized laccase, we employed the oxidation of ABTS by laccase to test laccase activity.[32] The specific activities of the free and immobilized laccase (at initial concentration of 3.0 mg/mL) in a phosphate buffer (pH 4.2, 30 °C) are given in Table 1. The laccase immobilized on the microspheres could retain a higher specific activity of 81.8% compared with other supports reported in previous literatures.[13,32] The further

Table 1. Activity of Free and Immobilized Laccase

laccase	immobilization capacity (mg/g)	specific activity (U/mg)	recovery yield (%)
free	–	13.2	100
immobilized	311.2	10.8	81.8

dx.doi.org/10.1021/sc400199v | ACS Sustainable Chem. Eng. 2014, 2, 396−403

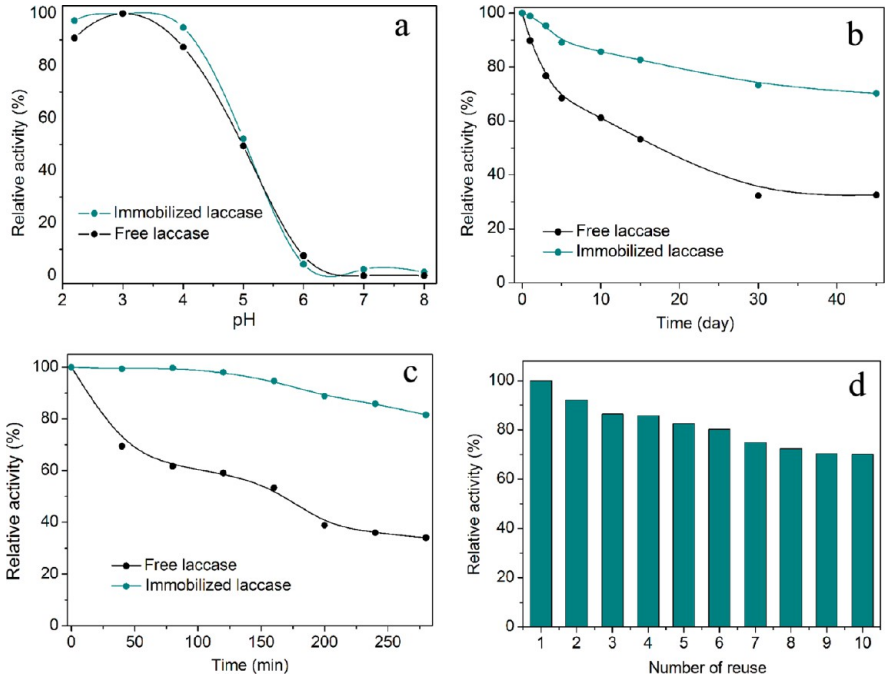

Figure 8. Properties of laccase. (a) Activity of free and immobilized laccase at different pH values. (b) Stability of free and immobilized laccase at 4 °C. (c) Activity of free and immobilized laccase as a function of time at 60 °C. (d) Reuse capacity of immobilized laccase.

experiments indicated that the immobilized urease and horseradish peroxidise on the microspheres also had a high specific activity of 86.5% and 78.6%, respectively. This indicates that the immobilization hardly caused the denature of the enzymes. ABTS can easily diffuse into the porous channels of supports and be oxidized by the immobilized enzymes. In addition, compared with other carriers made of natural clays, the microspheres also have higher loading capacity and enzyme activity.[13]

The activity of the free and immobilized laccase was also evaluated at varied conditions (Figure 8). The activity of the free and immobilized laccase as a function of pH values is shown in Figure 8a. Both the free and immobilized laccase exhibit maximal activity at pH 3.2 and lost almost all activity above pH 6.0. Compared with the free laccases, the immobilized laccase shows slightly higher adaptability to changes in pH of the medium below pH 5.0.

The stability over time and under thermal conditions is another important factor for immobilized enzymes. The storage stability of free and immobilized laccase were compared in phosphate buffer (0.1 M, pH 4.2) at 4 °C for a predetermined period of time. As shown in Figure 8b, the activity of free laccase, under the same storage condition, drop much faster over time than that of the immobilized laccase. The immobilized laccase still retains around 75% of its original activity in the buffer solution after 50 days. In contrast, the free laccase only maintained ~32% of its original activity over the same period.

To further investigate the time-dependent thermal stability of the immobilized laccase, the free and immobilized laccases were handled at a constant temperature of 60 °C in a buffer solution of pH 4.2 for varied incubation periods (Figure 8c). The activity of the immobilized laccase decreased much more slowly than that of the free laccase. The remaining activities of the free laccase and immobilized laccase were 32.2% and 82.6%, respectively, after an incubation period of 4 h. This is unambiguous evidence to address the advantages of an immobilized enzyme in thermal stability.

Unlike the free enzyme, the immobilized enzyme could be easily recovered from the solution after reaction, which greatly decreased the cost of the enzyme for practical applications. After every cycle of the reaction with the laccase immobilized on the porous microspheres, the reaction mixture was centrifuged to remove the supernatant. The microspheres were repeatedly water washed several times, and the activity of laccase was assayed (Figure 8d). More than 70% of initial activity was retained after 10 cycles. It indicates that the enzyme could be immobilized firmly within the porous microspheres and not leached from the pore channels. In contrast, the free enzyme could not be reused.

The comparison in activity of the free and immobilized laccase explicitly indicated that the biomimetic porous microsphere is an excellent support for enzyme immobilization. The nest-like microsphere was constructed from lapped halloysite nanotubes, which formed interconnected pore channels on both the micro- and nanometer scales. Those structural properties endow easier substrate accessibility to the immobilized enzyme molecules during enzyme-promoted reactions, reducing or eliminating mass-transfer barriers of substrates and thus enhancing the enzyme activity. The porous microspheres could provide a favorable environment for achieving high enzyme activity, significantly improved storage and recycling stability.

The immobilization and distribution of laccase enzyme in the porous microspheres were further examined by a fluorescence microscope. For the purpose of fluorescent imaging, the fluorescein isothiocyanate (FITC) labled-laccase was used. Each individual microsphere displays in a bright green color in whole (Figure 9), suggestive of the homogeneous immobilization of laccase on and within the microspheres. The spherical morphology stays unaltered after loading of laccase. Also, the

dx.doi.org/10.1021/sc400199v | ACS Sustainable Chem. Eng. 2014, 2, 396−403

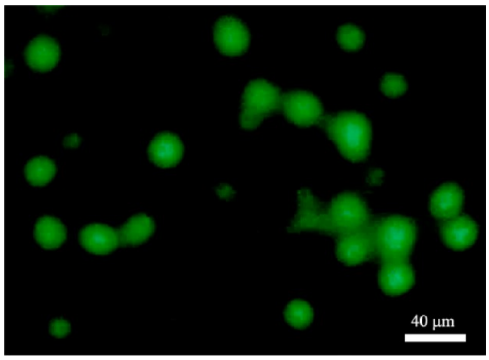

Figure 9. Fluorescence microscope image of microspheres immobilized by FITC-labeled laccase.

microspheres loaded with laccase show excellent dispersion without a significant agglomeration.

The FTIR spectra reveal the immobilization of laccase onto the microspheres (Figure S6, Supporting Information). The attachment of dopamine to the microspheres was confirmed from the characteristic C−H and carbonyl stretching vibrations peaked at 2925 and 1709 cm^{-1}, respectively.[26] After the loading of laccase, the characteristic bands at 1638 and 1411 cm^{-1} show a slight shift of about 10 cm^{-1} to a lower frequency, indicative of the interaction between laccase and functional groups of poly(dopamine) on the surface of microspheres. The FTIR characterization confirms that laccase keeps its essential structure after immobilization. Furthermore, the immobilization is of high stability, and the loss of laccase is hardly found during the entire experiments.

CONCLUSIONS

We prepared biomimetic porous microspheres of self-assembled HNTs using all natural molecules and a clay mineral without any toxic components and tedious procedures. An electrostatic interaction mechanism was proposed to demonstrate the assembly occurred in environmentally benign solution conditions. The microspheres, as highly biocompatible carriers, show superiority over other synthetic supports for biomolecule immobilization. The large mesopore, hierarchical pore distribution, and poly(dopamine) modification lead to a significantly enhanced capacity as high as 311.2 mg/g for laccase loading. The specific activity of ∼80% can be retained for the immobilized laccase. Furthermore, the microspheres showed excellent thermal and recycle use stability. It is expected that the biomimetic microspheres can be used as biologically safe and chemically stable microcapsules for immobilizing a variety of biomacromolecules. The method for microsphere preparation can be very promising for practical applications due to its capability in scalable production and green operation.

ASSOCIATED CONTENT

Supporting Information

Pore size distribution of the porous microspheres and XPS and FTIR spectra of the samples. This material is available free of charge via the Internet at http://pubs.acs.org.

AUTHOR INFORMATION

Corresponding Author

*E-mail: zhangb@zzu.edu.cn (B.Z.); xiangxu@mail.buct.edu.cn (X.X.).

Notes

The authors declare no competing financial interest.

ACKNOWLEDGMENTS

The authors acknowledge the financial support from the National Natural Science Foundation of China (Grant no. 21271158 and 21076016) and the fund of State Key Laboratory of Chemical Resource Engineering (BUCT).

REFERENCES

(1) Hofmann, U. On the chemistry of clay. *Angew. Chem., Int. Ed.* **1968**, *1*, 9681−692.

(2) Foresti, E.; Hochella, M. F.; Konishi, H.; Lesci, I. G.; Madden, A. S.; Roveri, N.; Xu, H. F. Morphological and chemical/physical characterization of Fe-doped synthetic chrysotile nanotubes. *Adv. Funct. Mater.* **2005**, *15*, 1009−1016.

(3) Guimaraes, L.; Enyashin, A. N.; Frenzel, J.; Heine, T.; Duarte, H. A.; Seifert, G. Imogolite nanotubes: Stability, electronic, and bechanical properties. *ACS Nano* **2007**, *1*, 362−368.

(4) Yah, W. O.; Atsushi, T.; Lvov, Y. Selective modification of halloysite lumen with octadecylphosphonic acid: New inorganic tubular micelle. *J. Am. Chem. Soc.* **2012**, *134*, 1853−1859.

(5) Su, D. H.; Wang, C. H.; Cai, S. M.; Mu, C. D.; Li, D. F.; Lin, W. Influence of palygorskite on the structure and thermal stability of collagen. *Appl. Clay Sci.* **2012**, *62*−*63*, 41−46.

(6) Lvov, Y.; Shchukin, D.; Möhwald, H.; Price, R. Halloysite clay nanotubes for controlled release of protective agents. *ACS Nano* **2008**, *2*, 814−820.

(7) Abdullayev, E.; Lvov, Y. Clay nanotubes for corrosion inhibitor encapsulation: release control with end stoppers. *J. Mater. Chem.* **2010**, *20*, 6681−6687.

(8) Dawson, J. I.; Kanczler, J. M.; Yang, X. B.; Attard, G. S.; Oreffo, R. O. C. Clay gels for the delivery of regenerative microenvironments. *Adv. Mater.* **2011**, *23*, 3304−3308.

(9) Liu, L.; Wan, Y. Z.; Xie, Y. D.; Zhai, R.; Zhang, B.; Liu, J. D. The removal of dye from aqueous solution using alginate-halloysite nanotube beads. *Chem. Eng. J.* **2012**, *187*, 210−216.

(10) Fix, D.; Andreeva, D.; Möhwald, H.; Lvov, Y.; Shchukin, D. Application of inhibitor loaded halloysite nanotubes in active anti-corrosive coatings. *Adv. Funct. Mater.* **2009**, *19*, 1720−1727.

(11) Zhai, R.; Zhang, B.; Liu, L.; Xie, Y. D.; Zhang, H. Q.; Liu, J. D. Immobilization of enzyme biocatalyst on natural halloysite nanotubes. *Catal. Commun.* **2010**, *12*, 259−263.

(12) Guo, M. Y.; Wang, A. F.; Muhammad, F.; Qi, W. X.; Ren, H.; Guo, Y. J.; Zhu, G. S. Halloysite nanotubes, a multifunctional nanovehicle for anticancer drug delivery. *Chin. J. Chem.* **2012**, *30*, 2115−2120.

(13) Durán, N.; Rosa, M. A.; D'Annibale, A.; Gianfreda, L. Applications of laccases and tyrosinases (phenoloxidases) immobilized on different supports: A review. *Enzyme Microb. Technol.* **2002**, *31*, 907−931.

(14) Prakasham, R. S.; Sarala, D. G.; Laxmi, K. R.; Rao, Ch. S. Novel synthesis of ferric impregnated silica nanoparticles and their evaluation as a matrix for enzyme immobilization. *J. Phys. Chem. C.* **2007**, *111*, 3842−3847.

(15) Hughes, A. D.; King, M. R. Use of naturally occurring halloysite nanotubes for enhanced capture of flowing cells. *Langmuir.* **2010**, *26*, 12155−12164.

(16) Kelly, H. M.; Deasy, P. B.; Ziaka, E.; Claffey, N. Formulation and preliminary in vivo dog studies of a novel drug delivery system for the treatment of periodontitis. *Inter. J. Pharmaceut.* **2004**, *274*, 167−183.

(17) Vergaro, V.; Abdullayev, E.; Lvov, Y.; Zeitoun, A.; Cingolani, R.; Rinaldi, R.; Leporatti, S. Cytocompatibility and uptake of halloysite clay nanotubes. *Biomacromolecules* **2010**, *11*, 820−829.

(18) Kim, J.; Lee, J.; Na, H. B.; Kim, B. C.; Youn, J. K.; Kwak, J. H.; Moon, K.; Lee, E.; Kim, J.; Park, J.; Dohnalkova, A.; Park, H. G.; Gu, M. B.; Chang, H. N.; Grate, J. W.; Hyeon, T. A. Magnetically

separable, highly stable enzyme system based on nanocomposites of enzymes and magnetic nanoparticles shipped in hierarchically ordered, mesocellular, mesoporous silica. *Small* **2005**, *1*, 1203−1207.
(19) Tortajada, M.; Ramón, D.; Beltránd, D.; Amorós, P. Hierarchical bimodal porous silicas and organosilicas for enzyme immobilization. *J. Mater. Chem.* **2005**, *15*, 3859−3868.
(20) Chen, L. H.; Zhu, G. S.; Zhang, D. L.; Zhao, H.; Guo, M. Y.; Wei, S. B.; Qiu, S. L. Novel mesoporous silica spheres with ultra-large pore sizes and their application in protein separation. *J. Mater. Chem.* **2009**, *19*, 2013−2017.
(21) Sun, J. M.; Zhang, H.; Tian, R. J.; Ma, D.; Bao, X. H.; Su, D. S.; Zou, H. F. Ultrafast enzyme immobilization over large-pore nanoscale mesoporous silica particles. *Chem. Commun.* **2006**, *43*, 1322−1324.
(22) Li, Z. Q.; Ding, Y.; Xiong, Y. J.; Yang, Q.; Xie, Y. One-step solution-based catalytic route to fabricate novel α-MnO_2 hierarchical structures on a large scale. *Chem. Commun.* **2005**, *7*, 918−920.
(23) Jun, S. H.; Lee, J. W.; Kim, B. C; Lee, J. E.; Joo, J.; Park, H.; Lee, J. H.; Lee, S. M.; Lee, D. H.; Kim, S. Y.; Koo, Y. M.; Shin, C. Ho.; Kim, S. W.; Hyeon, T. W.; Kim, J. B. Highly efficient enzyme immobilization and stabilization within meso-structured onion-like silica for biodiesel production. *Chem. Mater.* **2012**, *24*, 924−929.
(24) Tazaki, K. Microbial formation of a halloysite-like Mineral. *Clay Clay Miner.* **2005**, *53*, 224−233.
(25) Lee, H.; Rho, J.; Messersmith, P. B. Facile conjugation of biomolecules onto surfaces via mussel adhesive protein inspired coatings. *Adv. Mater.* **2009**, *21*, 431−434.
(26) Yah, W. O.; Xu, H.; Soejima, H.; Ma, W.; Lvov, Y.; Takahara, A. Biomimetic dopamine derivative for selective polymer modification of halloysite nanotube lumen. *J. Am. Chem. Soc.* **2012**, *134*, 12134−12137.
(27) Lee, H.; Dellatore, S. M.; Miller, W. M.; Messersmith, P. B. Mussel-inspired surface chemistry for multifunctional coatings. *Science* **2007**, *318*, 426−430.
(28) Ye, Q.; Zhou, F.; Liu, W. Bioinspired catecholic chemistry for surface modification. *Chem. Soc. Rev.* **2011**, *40*, 4244−4258.
(29) Ochs, C. J.; Hong, T.; Such, G. K.; Cui, J.; Postma, A.; Caruso, F. Dopamine-mediated continuous assembly of biodegradable capsules. *Chem. Mater.* **2011**, *23*, 3141−3143.
(30) Jan, J. S.; Shantz, D. F. Biomimetic silica formation: Effect of block copolypeptide chemistry and solution conditions on silica nanostructure. *Adv. Mater.* **2007**, *19*, 2951−2956.
(31) Ejima, H.; Richardson, J. J.; Caruso, F. Multivalent directed assembly of colloidal particles. *Angew. Chem., Int. Ed.* **2013**, *52*, 3314−3316.
(32) Zhu, Y.; Kaskel, S.; Shi, J.; Wage, T.; van, Pée, K. H. Immobilization of *Trametes versicolor* laccase on magnetically separable mesoporous silica spheres. *Chem. Mater.* **2007**, *19*, 6408−6413.
(33) Levis, S. R.; Deasy, P. B. Characterisation of halloysite for use as a microtubular drug delivery system. *Int. J. Pharmaceut.* **2002**, *243*, 125−134.
(34) Mellouk, S.; Cherifi, S.; Sassi, M.; Marouf-Khelifa, K.; Bengueddach, A.; Schott, J.; Khelifa, A. Intercalation of halloysite from Djebel Debagh (Algeria) and adsorption of copper ions. *Appl. Clay Sci.* **2009**, *44*, 230−236.
(35) Mesquita, J. P.; Donnici, C. L.; Pereira, F. V. Biobased nanocomposites from layer-by-layer assembly of cellulose nanowhiskers with chitosan. *Biomacromolecules* **2010**, *11*, 473−480.
(36) Chen, H. G.; He, J. H. Facile Synthesis of monodisperse manganese oxide nanostructures and their application in water treatment. *J. Phys. Chem. C.* **2008**, *112*, 17540−17545.
(37) Panhuis, M. I. H.; Paunov, V. N. Assembling carbon nanotubosomes using an emulsion- inversion technique. *Chem. Commun.* **2005**, *42*, 1726−1728.
(38) Wang, G. H.; Sun, Q.; Zhang, R.; Li, W. C.; Zhang, X. Q.; Lu, A. H. Weak acid−base interaction induced assembly for the synthesis of diverse hollow nanospheres. *Chem. Mater.* **2011**, *23*, 4537−4542.
(39) Wang, W. C.; Jiang, Y.; Wen, S. P.; Liu, L.; Zhang, L. Q. Preparation and characterization of polystyrene/Ag core−shell microspheres: A bio-inspired poly(dopamine) approach. *J. Colloid Interface Sci.* **2012**, *368*, 241−249.
(40) Burzio, L. A.; Waite, J. H. Cross-linking in adhesive quinoproteins: Studies with model decapeptides. *Biochemistry* **2000**, *39*, 11147−11153.
(41) Leeden, M. C. Are conformational changes, induced by osmotic pressure variations, the underlying mechanism of controlling the adhesive activity of mussel adhesive proteins? *Langmuir* **2005**, *21*, 11373−11379.
(42) Ni, K. F.; Lu, H. M.; Wang, C. X.; Black, K. C. L.; Wei, D. Z.; Ren, Y. H.; Messersmith, P. B. A novel technique for in situ aggregation of *Gluconobacter oxydans* using bio-adhesive magnetic nanoparticles. *Biotechnol. Bioeng.* **2012**, *109*, 2970−2977.
(43) Lee, H.; Scherer, N. F.; Messersmith, P. B. Single-molecule mechanics of mussel adhesion. *Proc. Natl. Acad. Sci. U.S.A.* **2006**, *103*, 12999−13003.
(44) Cui, J. W; Yan, Y.; Such, G. K.; Liang, K.; Ochs, C. J.; Postma, A.; Caruso, F. Immobilization and intracellular delivery of an anticancer drug using mussel-inspired polydopamine capsules. *Biomacromolecules* **2012**, *13*, 2225−2228.
(45) Pan, F. S.; Jia, H. P.; Qiao, S. Z.; Jiang, Z. Y.; Wang, J. T.; Wang, B. Y.; Zhong, Y. R. Bioinspired fabrication of high performance composite membranes with ultrathin defect-free skin layer. *J. Membr. Sci.* **2009**, *341*, 279−285.
(46) Qiu, H.; Xu, C.; Huang, X.; Ding, Y.; Qu, Y.; Gao, P. Immobilization of laccase on nanoporous gold: comparative studies on the immobilization strategies and the particle size effects. *J. Phys. Chem. C.* **2009**, *113*, 2521−2525.
(47) Arica, M. Y.; Altintas, B.; Bayramoglu, G. Immobilization of laccase onto spacer-arm attached non-porous poly(GMA/EGDMA) beads: Application for textile dye degradation. *Bioresour. Technol.* **2009**, *100*, 665−669.
(48) Kunamneni, A.; Ghazi, I.; Camarero, S.; Ballesteros, A.; Plou, F. J.; Alcalde, M. Decolorization of synthetic dyes by laccase immobilized on epoxy-activated carriers. *Process Biochem.* **2008**, *43*, 169−178.
(49) Wang, F.; Guo, C.; Yang, L. R.; Liu, C. Z. Magnetic mesoporous silica nanoparticles: Fabrication and their laccase immobilization performance. *Bioresour. Technol.* **2010**, *101*, 8931−89.